THE ASTROPHYSICAL JOURNAL, 464:L55–L58, 1996 June 10

CONTINUUM VLBI POLARIMETRY OF 3C 454.3 AT 43 GHz

A. J. KEMBALL AND P. J. DIAMOND
National Radio Astronomy Observatory, P.O. Box 0, Socorro, NM 87801

AND

I. I. K. PAULINY-TOTH
Max-Planck-Institut für Radioastronomie, Auf dem Hügel 69, D-53121 Bonn, Germany
Received 1996 February 8; accepted 1996 March 25

ABSTRACT

We present 43 GHz VLBA polarization observations of the quasar 3C 454.3 and discuss technical aspects concerning the calibration of millimeter VLBI polarimetry. Significant polarization fine structure is observed near the core of 3C 454.3, with a predominant electric field vector orientation parallel to the projected jet direction. This contrasts with previous centimeter VLBI polarimetry of quasars for which an orthogonal polarization orientation is generally found on larger VLBI scales.

Subject headings: galaxies: individual (3C 454.3) — galaxies: jets — polarization

1. INTRODUCTION

The use of very long baseline interferometry (VLBI) to image the linearly polarized radio emission in compact extragalactic radio sources has provided unique insights into the magnetic field distribution in these objects at milliarcsecond resolution. There has been extensive work done using this technique, from the first application (Cotton et al. 1984; Wardle et al. 1986) through the present (Wardle & Roberts 1994 and references therein). Polarization VLBI illuminates inherent physical differences in source properties that may otherwise not be discernible in total intensity VLBI observations. In particular, existing work at centimeter wavelengths (5–8 GHz) has shown a clear dependence on optical class of the orientation of the electric field vector with respect to the underlying jet axis (Gabuzda et al. 1992; Cawthorne et al. 1993). In BL Lac objects the electric field vector is found to lie parallel to the jet axis, while in quasars the orientation is perpendicular to the jet axis. In contrast, the polarization orientation of the core components is randomly distributed with no clear dependence on optical class (Gabuzda 1992). Several explanations have been proposed for the latter property, including the possible predominance of local Faraday depolarization in the core, the presence of small-scale jet curvature, or the blending of emerging jet components (Gabuzda 1992; Cawthorne et al. 1993). This question can only be addressed through high-resolution VLBI polarimetry at high frequencies.

Polarization calibration at high frequencies has traditionally been difficult due to poor sensitivity and high antenna instrumental polarization across inhomogeneous networks. The higher observing frequency and increased spatial resolution diminish the chances of finding ideal VLBI polarization calibrators. These include ultracompact linearly polarized sources or sources with negligible linear polarization but more extended structure. The advent of the Very Long Baseline Array (VLBA), which has standardized feeds with low instrumental polarization, has minimized these observational difficulties. Recent work in polarization calibration has suggested that somewhat resolved sources may be used in an iterative polarization calibration scheme (Cotton 1993). A full generalization of this method has been developed by Leppänen, Zensus, & Diamond (1995) in calibrating 22 GHz polarization observations with the VLBA. The latter technique does not require iteration and is insensitive to structure in the polarization calibrator. The use of maser sources in polarization calibration has been considered by Kemball, Diamond, & Cotton (1995).

In this Letter we present a polarization image of the quasar 3C 454.3 at 7 mm wavelength using data obtained with the VLBA. This strong radio source at a redshift $z = 0.859$ is an optically violent variable and is classified as a high optical polarization ($p > 3\%$) quasar. It has been the subject of extensive VLBI observations (Pauliny-Toth et al. 1987 and references therein). This work is part of an ongoing effort to evaluate polarization calibration techniques for millimeter VLBI polarimetry.

The data reduction methods used for polarization calibration at this frequency are described, and the astrophysical interpretation of the submilliarcsecond polarization structure is discussed. Section 2 contains a description of the observations and data reduction methods. The results and discussion are presented in § 3.

2. OBSERVATIONS AND DATA REDUCTION

The observations were conducted on 1994 December 1, from 23:00 to 12:00 UT the following day using the full VLBA. Good data were obtained from all stations except Fort Davis. The data were recorded in 1 bit VLBA format with 16 MHz per circular polarization, comprising four base-band converters of 4 MHz bandwidth each. The representative system temperature for each 25 m antenna was ~150 K, with a point-source sensitivity of ~11 Jy K^{-1}. The source 3C 454.3 was observed for a total of 4 hr, and 0420−014, a candidate polarization calibrator, for approximately 2 hr. Spectral-line sources were observed for the remaining time. The geometric mean of the synthesized beamwidth in natural weighting was ~300 μas. The data were correlated at the VLBA correlator in Socorro, New Mexico, operated by the National Radio Astronomy Observatory.[1]

[1] The National Radio Astronomy Observatory (NRAO) is operated by Associated Universities, Inc., under cooperative agreement with the National Science Foundation.

The data were reduced within the Astronomical Image Processing System (AIPS) maintained by NRAO, and a brief description of the data reduction path is given here. Corrections were applied for known digital processing effects within the VLBA correlator, and the data edited using VLBA monitor data and by inspection. Amplitude calibration was performed using measured system temperatures in each 4 MHz base band and recent gain information for each antenna. A solution was made for the opacity correction at each antenna as a function of time by solving for receiver temperature and zenith opacity, assuming a sec z dependence of atmospheric path length, and using an empirical expression for the relation between atmospheric and ground temperatures. The cross-power bandpass response in each base band was modeled as a complex Chebyshev polynomial expansion and determined in a fit that accounted for the manner in which antenna-based fringe rotation is performed in the VLBA correlator. Fringe fitting in residual delay and fringe rate was performed for the parallel-hand data using the Cotton-Schwab algorithm (Schwab & Cotton 1983), and the cross-hand fringes referred to the same frame by measuring and correcting for the differential polarization delay and phase at the reference antenna. The absolute phase offset between right-circular polarization and left-circular polarization at the reference antenna was determined from VLA observations of the continuum source 0420−014 on 1994 November 12. An independent estimate of the phase difference was obtained from the polarization spectrum of the 43 GHz SiO maser emission toward the late-type star VY CMa, which was observed as part of both the VLA and the VLBI observing runs. The two measurements agreed within 7°.5. The absolute polarization position angles are referenced to an assumed polarization position angle for 3C 286 of 33°.

Both 0420−014 and 3C 454.3 were mapped using iterative self-calibration and CLEAN deconvolution in the standard manner. Images of both sources in Stokes Q and U were produced after instrumental polarization calibration using standard half-plane Hermitian imaging techniques. The sampling in RL and LR was sufficiently uniform so as not to require complex polarization imaging in Q and U.

As part of this work, the source 0420−014 was used as an iterative polarization calibrator under the similarity approximation developed by Cotton (1993) discussed above. This source was chosen as a candidate polarization calibrator due to its compact structure in previous millimeter VLBI observations (Krichbaum et al. 1993). In the similarity method, the linearly polarized emission is assumed to be a scaled form of the underlying total intensity emission. The accuracy of this approximation can be improved by iterative polarization self-calibration (Cotton 1993). On each iteration, the current linearly polarized model in Stokes Q and U is subtracted from the amplitude- and phase-calibrated visibility data, and a new solution is obtained for the antenna-based instrumental polarization using the similarity approximation. This method converged rapidly when applied to 0420−014, reducing the off-source rms noise in the linearly polarized intensity image by a factor of ~2.6 within two iterations. The polarization calibration method evaluated here appears to work adequately for a source of this flux density when observed with a network with low instrumental polarization, such as the VLBA. Measured feed D terms (Kemball et al. 1995) were found to be of the order of a few percent uniformly across the array. The polarization structure of 0420−014 is shown in Figure 1, where

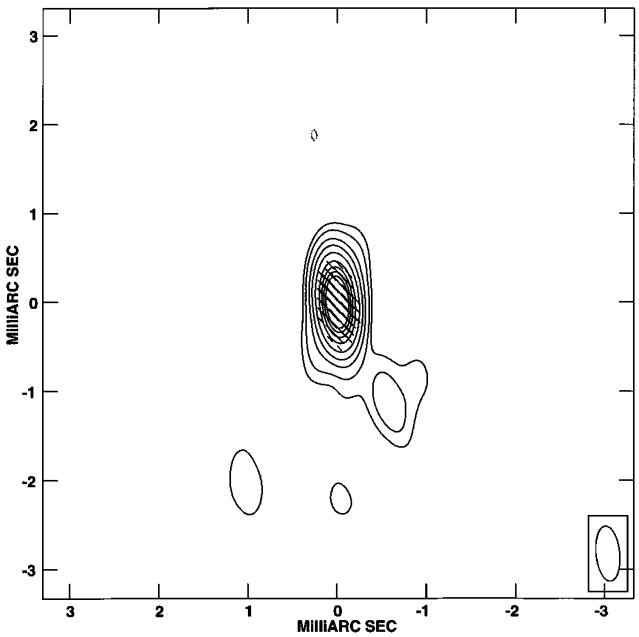

FIG. 1.—VLBI polarization map of 0420−014 at 43 GHz. Stokes I is plotted as a contour map with levels of 15 mJy beam^{-1} times (−10, −5, −2, −1, 1, 2, 5, 10, 20, 40, 60, 80, 100, and 200). The vectors indicate the plane of the electric field vector and have a length proportional to the linearly polarized intensity, where 1 mas = 256 mJy beam^{-1}.

the distribution of the polarization position angle is shown superimposed on a contour plot of the total intensity I. The vectors denote the plane of the electric field vector, with the length of the vector proportional to the linearly polarized intensity $P = (Q^2 + U^2)^{1/2}$. There is some extension in the total intensity image, but the polarized emission is confined strongly to a compact core, thus allowing the successful application of this approximation. The peak percentage linear polarization is $p \sim 4.3\%$.

3. RESULTS AND DISCUSSION

The VLBI polarization map obtained for 3C 454.3 is shown in Figure 2. The Stokes I map consists of two dominant components separated by 0.6 mas (2.5 h^{-1} pc) at a position angle of −65°. The components will be referred to as 1 and 2, numbered from east to west. A model fit assuming two elliptical Gaussian components in the I image yielded nominal component sizes and orientations of 0.38×0.078 mas, P.A. = 124° and 0.31×0.20 mas, P.A. = 148°, respectively. The flux densities were measured as $S_1 \sim 3.4$ Jy and $S_2 \sim 3.7$ Jy, respectively, subject to an estimated uncertainty in the absolute flux density scale of ~10%.

The maxima in linearly polarized emission do not coincide exactly with the I component positions, and estimates of the percentage linear polarization for each component derived from integrated image measurements are uncertain as a result. Peak percentage polarization measurements were adopted accordingly, with the peak component position defined by the linearly polarized emission. Components 1 and 2 have counterparts in the P image, but there is further evidence for an intermediate linearly polarized feature (1a) in P at a separation of ~0.27 mas (1.1 h^{-1} pc) from component 1. A nearby feature is recovered when fitting three components in the I image, but this association is not unambiguous. The peak per-

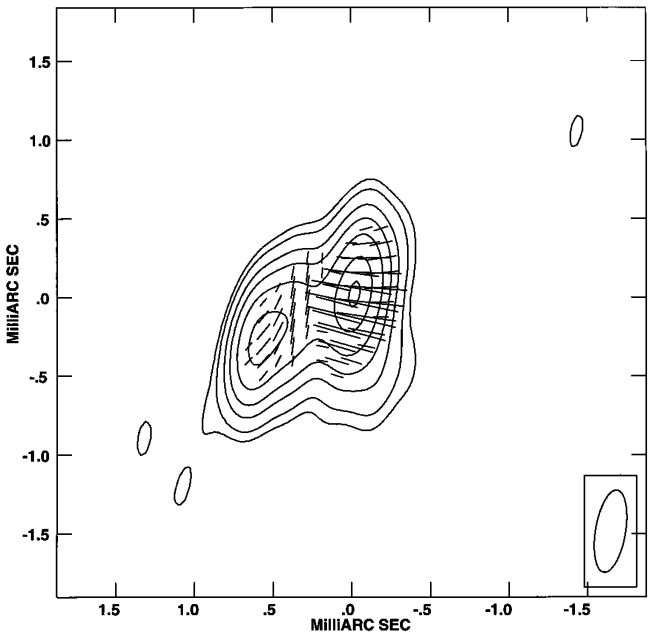

FIG. 2.—VLBI polarization map of 3C 454.3 at 43 GHz. Stokes I is plotted as a contour map with levels of 35 mJy beam^{-1} times (-10, -5, -2, -1, 1, 2, 5, 10, 20, 40, and 60). The vectors indicate the plane of the electric field vector and have a length proportional to the linearly polarized intensity, where 1 mas = 256 mJy beam^{-1}.

centage linear polarizations of each of the dominant components in the P image are given by $p_1 \sim 2\%$, $p_{1a} \sim 4\%$, and $p_2 \sim 7\%$, when measured as described above.

The polarization position angle varies considerably between the individual polarized features, with 90° difference between the polarization position angles of components 1a and 2. The integrated rotation measure for 3C 454.3 has been measured as -57 rad m^{-2} (Broten, Macleod, & Vallée 1988) and -44 rad m^{-2} (Simard-Normandin, Kronberg, & Button 1981). No correction has accordingly been made for integrated Faraday rotation.

The quasar 3C 454.3 has been the subject of extensive VLBI observations (Pauliny-Toth et al. 1987) and has a known core-jet morphology at a dominant position angle of $-65°$ (Padrielli et al. 1986). There is a break in the apparent jet direction within a few milliarcseconds of the core, where the dominant projected jet position angle lies between $-95°$ and $-105°$, as shown in 8 and 22 GHz VLBI observations (Pauliny-Toth et al. 1987; Charlot 1990). Component 1 in Figure 2 is identified as the core (Pauliny-Toth et al. 1987). In the 43 GHz maps presented here, component 2 appears at a comparable separation from the core as the closest inner jet component visible in previous 10.7 GHz observations (Pauliny-Toth et al. 1987), but at a differing position angle. This feature, which shows no significant apparent transverse motion at 10.7 GHz, has been postulated as a stationary shock (Pauliny-Toth et al. 1987).

Integrated polarization measurements at 33.5 GHz (Flett & Henderson 1983) show variability about a mean polarization $\bar{p} = 4.5\%$. Multifrequency integrated measurements by Jones et al. (1985) have previously shown a break in the polarization position angle near ~15 GHz, with data below and above this frequency showing, respectively, perpendicular and parallel orientation to the jet axis. Polarization VLBI observations of 3C 454.3 at 5 GHz (Cawthorne & Gabuzda 1996) indicate that the VLBI jet component polarization position angles are consistently orthogonal to the local jet direction. Since these components are optically thin, an axial magnetic field geometry is implied in the VLBI jet. From VLBI at frequencies $\leq$5 GHz, however, there is evidence that the polarization position angle becomes more parallel to the jet axis very close to the core (Cawthorne & Gabuzda 1996; Cotton et al. 1984).

The interpretation of the 43 GHz polarization images presented here would be aided by simultaneous VLBI polarimetry in an adjacent frequency band to measure local Faraday rotation and the spectral indices of the polarized components. It is clear, however, that there is significant polarization fine structure near the core, with evidence for possible emerging components (1a) and changes in the projected jet direction in the inner core region. These factors suggest that spatial blending may be partly responsible for the low core polarization observed for quasars in centimeter VLBI polarimetry (Cawthorne et al. 1993). The integrated percentage linear polarization derived from the VLBI map presented here is $\leq$2%. The low 43 GHz polarization observed for component 1 is consistent with its identification as the core. Component 2 appears to be associated with the stationary feature seen in 10.7 GHz VLBI maps. If these components are associated, the origin of the position angle difference is not clear. In this regard, recent 86 GHz VLBI observations at epochs 1993.3 and 1994.0 (Krichbaum et al. 1995) show a similar inner jet position angle to the 43 GHz data presented here. Single-dish monitoring (University of Michigan 1995) indicates an outburst that peaked at 5–8 GHz around 1994.4.[2] Component 1a may result from that outburst.

At 7 mm, the electric field vector is predominantly oriented parallel to the local projected jet direction. Between the core and component 2, however, the electric field vector is orthogonal. The predominant east-west electric field vector orientation may suggest a transverse compressed symmetry for the magnetic field geometry near the core (Jones et al. 1985) and stands in contrast to the expected orthogonal orientation found for most quasars in centimeter VLBI polarimetry. It does agree, however, with the recent result by Leppänen et al. (1995), who find a similar electric field vector orientation at 22 GHz near the core of the quasar 3C 345. The change in polarization position angle along the inner jet observed in 3C 454.3 at 43 GHz may result from either true changes in the local magnetic field direction (with parallel or perpendicular orientation dependent on opacity), a helical jet geometry, or the presence of local differential Faraday rotation. It is unlikely, however, that there is sufficient opacity in the jet components to rotate the apparent polarization position angle by 90°. It is noted that components 1 and 1a lie within the nominal linear scale for the broad-line region. If transverse shocks are present in quasars, they are most likely strongest near the core, and the change in the polarization position vector near the core finds a ready explanation. The polarization properties of component 1a may suggest that it is a weaker shock and that the underlying longitudinal field is established very early in the jet. Further observations are needed to confirm this.

We would like to thank C. Flatters for valuable discussions, and an anonymous referee for useful suggestions.

[2] This research has made use of data from the University of Michigan Radio Astronomy Observatory, which is supported by the National Science Foundation and by funds from the University of Michigan.

REFERENCES

Broten, N. W., Macleod, J. M., & Vallée, J. P. 1988, Ap&SS, 141, 303
Cawthorne, T. V., Wardle, J. F. C., Roberts, D. H., & Gabuzda, D. C. 1993, ApJ, 416, 519
Cawthorne, T. V., & Gabuzda, D. C. 1996, MNRAS, 278, 861
Charlot, P. 1990, A&A, 229, 51
Cotton, W. D., Geldzahler, B. J., Marcaide, J. M., Shapiro, I. I., Sanroma, M., & Ruis, A. 1984, ApJ, 286, 503
Cotton, W. D. 1993, AJ, 106, 1241
Flett, A. M., & Henderson, C. 1983, MNRAS, 204, 1285
Gabuzda, D. C. 1992, in Extragalactic Radio Sources—From Beams to Jets, ed. J. Roland et al. (Cambridge: Cambridge Univ. Press), 145
Gabuzda, D. C., Cawthorne, T. V., Roberts, D. H., & Wardle, J. F. C. 1992, ApJ, 388, 40
Jones, T. W., Rudnick, L., Aller, H. D., Aller, M. F., Hodge, P. E., & Fieldler, R. L. 1985, ApJ, 290, 627
Kemball, A. J., Diamond, P. J., & Cotton, W. D. 1995, A&A, 110, 383
Krichbaum, T. P., et al. 1993, A&A, 275, 375
Krichbaum, T. P., Britzen, S., Standke, S., Witzel, A., Schalinski, C. J., & Zensus, J. A., 1995, Proc. Natl. Acad. Sci., 92, 11377
Leppänen, K. J., Zensus, J. A., & Diamond, P. J. 1995, AJ, 110, 2479
Padrielli, L., et al. 1986, A&A, 165, 53
Pauliny-Toth, I. I. K., Porcas, R. W., Zensus, J. A., Kellermann, K. I., Wu, S. Y., Nicolson, G. D., & Mantovani, F. 1987, Nature, 328, 778
Schwab, F. R., & Cotton, W. D. 1983, AJ, 88, 688
Simard-Normandin, M., Kronberg, P. P., & Button, S. 1981, ApJS, 45, 97
University of Michigan 1995, University of Michigan Radio Astronomy Observatory Database, http://www.astro.lsa.umich.edu/obs/radiotel/umrao.html
Wardle, J. F. C., Roberts, D. H., Potash, R. I., & Rogers, A. E. E. 1986, ApJ, 304, L1
Wardle, J. F. C., & Roberts, D. H. 1994, in Compact Extragalactic Radio Sources, ed. J. A. Zensus & K. I. Kellermann (Socorro: NRAO), 217